Trajectory Tracking Control for a 3-DOF Parallel Manipulator Using Fractional-Order PI$^{\lambda}$D$^{\mu}$ Control

Ahmet Dumlu, *Member, IEEE*, and Koksal Erenturk, *Member, IEEE*

***Abstract*—In this paper, a 3-degrees-of-freedom parallel manipulator developed by Tsai and Stamper known as the Maryland manipulator is considered. In order to provide dynamic analysis, three different sequential trajectories are taken into account. Two different control approaches such as the classical proportional–integral–derivative (PID) and fractional-order PID control are used to improve the tracking performance of the examined manipulator. Parameters of the controllers are determined by using pattern search algorithm and mathematical methods for the classical PID and fractional-order PID controllers, respectively. Design procedures for both controllers are given in detail. Finally, the corresponding results are compared. Performance analysis for both of the proposed controllers is confirmed by simulation results. It is observed that not only transient but also steady-state error values have been reduced with the aid of the PI$^{\lambda}$D$^{\mu}$ controller for tracking control purpose. According to the obtained results, the fractional-order PI$^{\lambda}$D$^{\mu}$ controller is more powerful than the optimally tuned PID for the Maryland manipulator tracking control. The main contribution of this paper is to determine the control action with the aid of the fractional-order PI$^{\lambda}$D$^{\mu}$ controller different from previously defined controller structures. The determination of correct and accurate control action has great importance when high speed, high acceleration, and high accuracy needed for the trajectory tracking control of parallel mechanisms present unique challenges.**

***Index Terms*—Fractional calculus, manipulators, parallel robots, proportional–integral–derivative control, robot control.**

I. Introduction

WITH THE recent advances in technology, the parallel manipulators became more attractive in industrial applications which need higher sensitivity and accuracy. The parallel manipulators are generally used in flight simulators [1], medical operations [2]–[5], machine tools [6]–[8], micromotion [9], pick-and-place operations in industry [10], [11], etc.

Parallel manipulators consist of a moving platform that is connected to a fixed base by several limbs or legs, and every limb is controlled by one actuator individually. This structure results in a closed-loop kinematic chain mechanism. In general, the closed-loop kinematic chain mechanism has more complicated forward kinematics as compared to the conventional open-loop kinematic chain mechanism. The kinematic and dynamic analyses of these types of mechanisms have been the focus of many research works [12]–[18].

Manuscript received December 13, 2012; revised June 4, 2013; accepted August 4, 2013. Date of publication August 16, 2013; date of current version January 31, 2014.

The authors are with the Department of Electrical and Electronics Engineering, College of Engineering, Ataturk University, Erzurum 25240, Turkey (e-mail: ahmetdumlu@atauni.edu.tr; erenturk@yahoo.com; keren@atauni.edu.tr).

Color versions of one or more of the figures in this paper are available online at http://ieeexplore.ieee.org.

Digital Object Identifier 10.1109/TIE.2013.2278964

In these types of parallel mechanisms, the actuators are connected to limbs or legs. This construction is called motor-mechanism coupling systems. The dynamic characteristic of the motor-mechanism coupling model is highly nonlinear. When high speed, high acceleration, and high accuracy are needed, the trajectory tracking control of parallel mechanisms presents unique challenges [19]. The high-precision motion of parallel manipulators depends not only on the position accuracy of each actuator but also on the position synchronization of all actuators [20]. Therefore, Su *et al.* [20] presented a synchronized control algorithm for the set point position control of parallel manipulators. Ren *et al.* [19] proposed the convex synchronized control which is based on the convex combination method to improving tracking accuracy.

Su *et al.* [21] used a nonlinear proportional integral derivative algorithm to synthesize the control law for enhanced performance in areas such as increased damping and reduced tracking error for a general 6-degrees-of-freedom (DOF) parallel manipulator. Ouyang *et al.* [22] presented the nonlinear proportional–derivative (PD) control of multi-degree-of-freedom parallel manipulator systems for a generic task. Müller and Hufnagel [23] applied a model-based control for a planar parallel mechanism which is an efficient formulation in terms of a set of independent joint coordinates. Ghorbel *et al.* [24] built and modeled a planar delta robot and used a PD control approach for the stability of the robot. Li and Wang [25] applied a neural network proportional–integral–derivative (PID) controller to improve the trajectory tracking performance of parallel robotic systems.

In spite of the new progress on control area, PID-type controllers are unquestionably the most commonly used control algorithm in industry due to their practicality [26]–[28]. Their relatively simple structures that can be easily implemented and the availability of well-established rules for tuning the parameters of the controllers are the main reasons for making them preferable in real-time applications.

In classical PID control, there exist four weaknesses such as error computation; noise degradation in the derivative control; oversimplification and the loss of performance in the control law in the form of a linear weighted sum; and complications brought by the integral control [29].

In order to enhance the robustness and performance of PID control systems, Podlubny has proposed a generalization of the PID controllers, namely, PI$^{\lambda}$D$^{\mu}$ controllers. In the proposed work, the improvement of the proposed controller has been provided by using an integrator of order λ and a differentiator of order μ (the orders λ and μ may assume real noninteger values) [26], [30].

Numerous design methodologies intended for PI$^{\lambda}$D$^{\mu}$ controllers are reported in the literature [26]–[40]. Among the many applications of fractional-order controllers to engineering problems, those to a flexible belt transmission [32], an active suspension system [33], [34], irrigation canals [35], [36], or the control of flexible robots [37], [38] can be mentioned. In addition, an introductory work is given for single input/single output fractional control [41]. In [41], design basis and basic mathematical consideration for fractional-order control are given with an illustrative example. Two design techniques for tuning the parameters of the controller are presented in [42]. In [26], [27], [43], and [44], applications of fractional-order controllers to different types of engineering problems are illustrated.

In this paper, a 3-DOF parallel manipulator developed by Tsai and Stamper [45] is introduced, and the mechanism and motor dynamic models are formulated first.

Second, in order to improve the tracking performance of the examined Maryland manipulator, different control approaches such as classical PID and fractional-order PID control approaches have been investigated. A pattern search optimization method has been employed to optimize the parameters of the classical PID controller, and the gains have been found.

Finally, three different sequential trajectories have been considered, and results have been obtained for both cases. Using the PI$^{\lambda}$D$^{\mu}$ controller, overshoot values have been eliminated for trajectory changes. Employing the PI$^{\lambda}$D$^{\mu}$ controller for tracking control purpose, not only transient but also steady-state error values have been reduced. In addition, the sum squared error (SSE) values between the desired and obtained torque values showed that the fractional-order PI$^{\lambda}$D$^{\mu}$ controller is more powerful than the optimally tuned PID for the Maryland manipulator tracking control. Obtained results are also given in both the graphical and the tabulated form.

The main contribution of this paper is to determine the control action with the aid of the fractional-order PI$^{\lambda}$D$^{\mu}$ controller different from previously defined controller structures. The determination of correct and accurate control action has great importance when high speed, high acceleration, and high accuracy needed for the trajectory tracking control of parallel mechanisms present unique challenges.

The organization of the rest of this paper can be summarized as follows. The system structure is presented in Section II. Section III introduces the parallel manipulator mechanism and motor dynamic models developed by Tsai and Stamper. Both control strategies using the classical PID and fractional-order PI$^{\lambda}$D$^{\mu}$ controllers are introduced in Section IV. Simulation results for both cases are illustrated in Section V, followed by the concluding remarks in Section VI.

II. System Description

Fig. 1 shows the manipulator known as the University of Maryland manipulator [46].

The manipulator consists of a fixed platform, a moving platform, and three identical limbs that connect the moving platform to the fixed platform. Each limb consists of an input link and a planar four-bar parallelogram (passive links). For each limb, the input and passive links and the two platforms are connected by three parallel revolute joints. Moreover, each four-bar parallelogram consists of four revolute joints. Input links that are individually manipulated by the motors (Inland T-515B dc torque motor) can actuate by the rotation of the motors. Therefore, it is possible for the moving platform to move with only three translational degrees of freedom effectively.

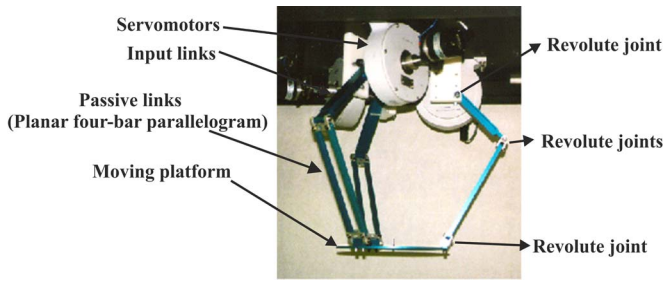

Fig. 1. University of Maryland manipulator [45].

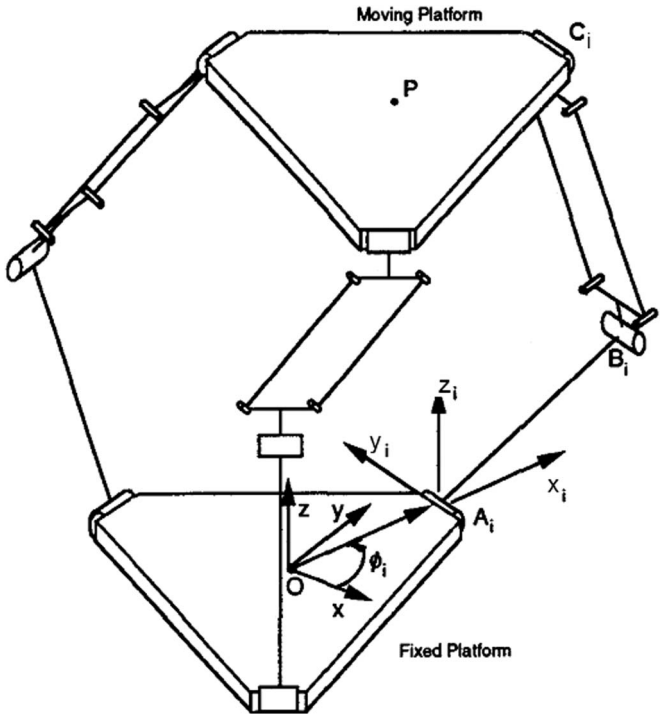

Fig. 2. Schematic diagram of manipulator [46].

III. Mathematical Model of Maryland Manipulator

A schematic diagram of the manipulator and the description of the joint angles are depicted in Figs. 2 and 3. In addition, the parameters of the manipulator are tabulated in Table I.

The points $A_i (i = 1, 2, 3)$ represent the summits of a fixed triangular platform. For the purpose of analysis, the reference coordinate system (x, y, z) to the fixed platform with its origin located at triangular center O and the z-axis perpendicular to the platform and the x–y-axes lies on a fixed plane.

The origin of this coordinate central system is located just at the center P of the moving triangle. Another coordinate system (x_i, y_i, z_i) is attached to the fixed platform at point A_i such that the x_i-axis is in-line with the extended line of OA_i, the y_i-axis

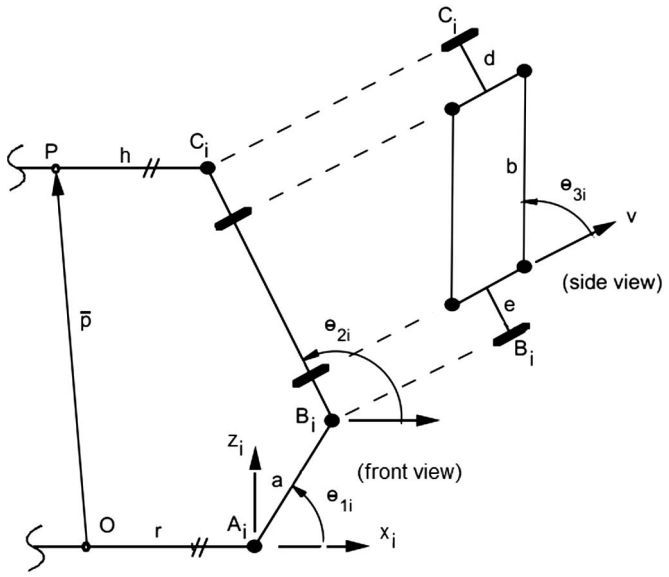

Fig. 3. Description of the joint angles [46].

TABLE I
PARAMETERS FOR MANIPULATOR

Symbol	Description	Value
θ_{1i}	actuator angle is measured from x_i axis to A_iB_i	find inverse kinematic (rad)
θ_{2i}	passive angle is defined from the extended line of A_iB_i to the line defined by the intersection of the plane of the parallelogram and the x_i-z_i plane	find inverse kinematic (rad)
θ_{3i}	passive angle is measured from the y_i direction to B_iC_i	find inverse kinematic (rad)
ϕ_i	angle is measured from the x-axis to the x_i –axis and is a constant parameter of the manipulator design.	[0,120,240] (deg)
a	length of links A_iB_i	203.2 mm
b	length of links B_iC_i	254.0 mm
e,d	small offset length of in parallelogram	0 mm → special form
r	radius of fixed platform	127.0 mm
h	radius of moving platform	127.0 mm
m_a	mass of the input link	0.184 kg
m_b	mass of the one of the two connecting rod	0.085 kg
m_p	mass of the moving platform	0.413 kg
I_m	axial moment of inertia of the rotor mounted on i*th* limb	0.00434 N.m.s^2

is directed along the revolute joint axis at A_i, and the z_i-axis is parallel to the z-axis.

If $d = e = 0$, a special case of the manipulator is formed. Therefore, this manipulator has a less complex kinematic structure and looks like a manipulator devised by Clavel [47] that employed spherical joints to obtain the desired kinematic structure. In order to simplify the analysis of the mathematical model of the manipulator, a special form of the manipulator is considered in this study.

For the parallel manipulators, inverse kinematics refers to the use of the kinematic equations of a manipulator to determine the joint parameters that provide a desired pose of the moving platform.

In order achieve this, a closed-loop equation can be written for each limb as

$$\overrightarrow{A_iB_i} + \overrightarrow{B_iC_i} = \overrightarrow{OP} + \overrightarrow{PC_i} - \overrightarrow{OA_i}. \tag{1}$$

Expressing (1) in the (x_i, y_i, z_i) coordinate frame, we obtain

$$\begin{bmatrix} a\cos(\theta_{1i}) + b\sin(\theta_{3i})\cos(\theta_{1i}+\theta_{2i}) \\ b\cos(\theta_{3i}) \\ a\sin(\theta_{1i}) + b\sin(\theta_{3i})\sin(\theta_{1i}+\theta_{2i}) \end{bmatrix} = \begin{bmatrix} c_{xi} \\ c_{yi} \\ c_{zi} \end{bmatrix} \tag{2}$$

where

$$\begin{bmatrix} c_{xi} \\ c_{yi} \\ c_{zi} \end{bmatrix} = \begin{bmatrix} \cos(\varnothing_i) & \sin(\varnothing_i) & 0 \\ -\sin(\varnothing_i) & \cos(\varnothing_i) & 0 \\ 0 & 0 & 1 \end{bmatrix} \begin{bmatrix} p_x \\ p_y \\ p_z \end{bmatrix} + \begin{bmatrix} h-r \\ 0 \\ 0 \end{bmatrix}. \tag{3}$$

Equation (3) denotes the position of point C_i relative to the (x_i, y_i, z_i) coordinate frame. Two solutions of θ_{3i} are found by solving the second element of (2)

$$\theta_{3i} = \pm\cos^{-1}\left(\frac{c_{yi}}{b}\right). \tag{4}$$

With θ_{3i} determined by using (4), an equation with θ_{2i} as the only unknown is generated by summing the squares of c_{xi}, c_{yi}, and c_{zi} in (2)

$$\theta_{2i} = \pm\cos^{-1}(k) \tag{5}$$

where $k = (c_{xi}^2 + c_{yi}^2 + c_{zi}^2 - a^2 - b^2)/(2ab\sin(\theta_{3i}))$.

By this way, corresponding to each solution set of θ_{2i} and θ_{3i}, (2) yields a unique solution for θ_{1i}.

Due to the complex kinematics of the manipulator, the equations of motion which describe the actuating torques are derived using the Lagrangian approach. The first type of Lagrange's equations will be employed by using three redundant coordinates, p_x, p_y, p_z and θ_{11}, θ_{12}, θ_{13}, as the generalized coordinates.

As proposed by Tsai [46], in order to simplify the analysis, we assume that the mass of each connecting rod, m_b, in the upper arm assembly is divided evenly and concentrated at the two endpoints B_i and C_i.

The total kinetic energy of the mechanism can be written as

$$T = \frac{1}{2}m_p\left(\dot{p}_x^2 + \dot{p}_y^2 + \dot{p}_z^2\right) + \frac{1}{2}\left(I_m + \frac{1}{3}m_a a^2\right)\dot{\theta}_{1i}^2 + \frac{1}{2}m_b\left(\dot{p}_x^2 + \dot{p}_y^2 + \dot{p}_z^2\right) + \frac{1}{2}m_b a^2\dot{\theta}_{1i}^2. \tag{6}$$

The total potential energy of the mechanism is given by

$$P = m_p g_c p_z + \frac{1}{2}m_a g_c a\sin(\theta_{1i}) + m_b g_c\left(p_z + a\sin(\theta_{1i})\right). \tag{7}$$

The Lagrangian equations of motion become

$$\frac{d}{dt}\left(\frac{\partial L}{\partial \dot{q}_i}\right) - \frac{\partial L}{\partial q_i} + \sum_{k=1}^{3}\lambda_k\frac{\partial \Gamma_k}{\partial q_i} = Q_i \qquad \text{for } i = 1 \text{ to } 6 \tag{8}$$

where

$$L = T - P \tag{9}$$

$$q_i = \begin{cases} p_x, p_y, p_z & i = 1,2,3 \\ \theta_{11}, \theta_{12}, \theta_{13} & i = 4,5,6 \end{cases} \tag{10}$$

$$Q_i = \begin{cases} F_i & i = 1,2,3 \\ T_{i-3} & i = 4,5,6 \end{cases} \tag{11}$$

and where F_i is the x-, y-, and z-components of an external force exerted on the moving platform and T_{i-3}, $i = 4,5,6$, denotes the frictional torques of the ith link in the θ_{1i}-direction.

The three constraint equations relating p_x, p_y, p_z and θ_{11}, θ_{12}, θ_{13} are obtained from the fact that the distance between joints B and C is always equal to the length of the connecting rod of the upper arm, b; that is

$$\Gamma_k = \overrightarrow{B_i C_i^2} - b^2 = 0. \tag{12}$$

The dynamic equation of the manipulator is then obtained as in the following form:

$$T_i = \frac{\partial}{\partial t}\left(\frac{\partial T}{\partial \dot{q}_i}\right) - \frac{\partial T}{\partial q_i} + \frac{\partial P}{\partial q_i} + \sum\nolimits_{k=1}^{3} \lambda_k \frac{\partial \Gamma_k}{\partial q_i} \tag{13}$$

where $i = 1, \ldots, 6$ and the three unknown Lagrangian multipliers λ_i can be solved from the three simultaneous equations, i.e., (8) with $i = 4,5,6$. Once the Lagrange multipliers are found, the actuator torques are obtained as follows:

$$\begin{aligned} \tau_1 = {} & \left(I_m + \frac{1}{3}m_a a^2 + m_b a^2\right)\ddot{\theta}_{11} \\ & + \left(\frac{1}{2}m_a + m_b\right) g_c\, a \cos(\theta_{11}) - 2a\lambda_1 \\ & \times [(p_x \cos(\varnothing_1) + p_y \sin(\varnothing_1) + h - r) \\ & \times \sin(\theta_{11}) - p_z \cos(\theta_{11})] \end{aligned} \tag{14}$$

$$\begin{aligned} \tau_2 = {} & \left(I_m + \frac{1}{3}m_a a^2 + m_b a^2\right)\ddot{\theta}_{12} \\ & + \left(\frac{1}{2}m_a + m_b\right) g_c\, a \cos(\theta_{12}) - 2a\lambda_2 \\ & \times [(p_x \cos(\varnothing_2) + p_y \sin(\varnothing_2) + h - r) \\ & \times \sin(\theta_{12}) - p_z \cos(\theta_{12})] \end{aligned} \tag{15}$$

$$\begin{aligned} \tau_3 = {} & \left(I_m + \frac{1}{3}m_a a^2 + m_b a^2\right)\ddot{\theta}_{13} \\ & + \left(\frac{1}{2}m_a + m_b\right) g_c\, a \cos(\theta_{13}) - 2a\lambda_3 \\ & \times [(p_x \cos(\varnothing_3) + p_y \sin(\varnothing_3) + h - r) \\ & \times \sin(\theta_{13}) - p_z \cos(\theta_{13})]. \end{aligned} \tag{16}$$

As can be seen from (14)–(16), the desired tracking control can be achieved by changing or controlling the supply voltage of the used motor. Three permanent magnet direct current (PMDC) motors have been used to get the linear relationship between the supply current and produced torque value.

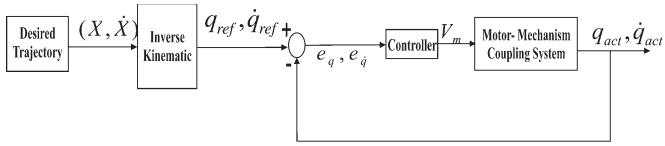

Fig. 4. Block scheme of general independent joint control.

The time domain equation of the PMDC motor, which is driving the manipulator load, can be written as follows:

$$\begin{bmatrix} \frac{di_a}{dt} \\ \frac{d\omega_m}{dt} \end{bmatrix} = \begin{bmatrix} -\frac{R_a}{L_a} & -\frac{K_v}{L_a} \\ \frac{K_t}{J_m} & -\frac{B_m}{J_m} \end{bmatrix} \begin{bmatrix} i_a \\ \omega_m \end{bmatrix} + \begin{bmatrix} \frac{V_a}{L_a} \\ -\frac{T_L}{J_m} \end{bmatrix} \tag{17}$$

where B_m is the damping coefficient ($0.07812\ \mathrm{N \cdot m \cdot s^{-1}}$), i_a is the motor current (no-load current $= 1.62$ A), J_m is the inertia of the rotor ($0.00434\ \mathrm{kg \cdot m^{-2}}$), K_v is the electro motor force constant (0.095) determined by the strength of the magnet, reluctance of iron, and number of turns of the armature winding, K_t is the torque constant, L_a is the armature inductance (0.00805 H), R_a is the armature resistance (1.4 Ω), T_L is the load torque ($\mathrm{N \cdot m}$), and V_a is the applied voltage to the motor (rated voltage $= 36$ V).

The T_L load torque value in (17) is equal to one of the τ_1, τ_2, or τ_3 given in (14)–(17) for the considered PMDC motor to get actuator torques.

On the other hand, from the torque equilibrium on the rotor

$$T = T_m - T_L - B\omega_a - J\dot{\omega}_a \tag{18}$$

is obtained. T_m in the equation represents the magnetic motor torque. As well known in a PMDC motor, field current is constant. The magnetic torque and the generated electromotive force for a given constant field current i_f are defined as

$$T_m = K_t i_a(t). \tag{19}$$

Combining (14)–(19), the load torque value for the tracking function has been acquired.

IV. Control Strategies

In this section, we present two control approaches, representing the classical PID and fractional-order PID control approaches, respectively, to investigate the effect of different control approaches on the improvement of the tracking performance of the examined Maryland manipulator. The block scheme of general independent joint control is shown in Fig. 4.

As can be seen from Fig. 4, both of the considered controllers are employed for the system with the same approach. For this reason, Fig. 4 can be used to illustrate both controller structures.

A. Classical PID

As a comparison, an optimally tuned PID controller is integrated to the system in the form of

$$V(t) = K_P e(t) + K_I \int e(t)dt + K_D \frac{de(t)}{dt} \tag{20}$$

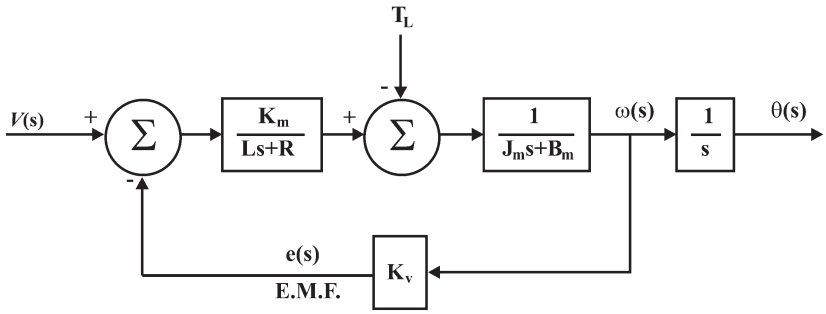

Fig. 5. Mathematical model of a dc motor in s-domain.

where K_P, K_I, and K_D represent the proportional, integral, and derivative gains, respectively. $e(t)$ denotes the error in the speed signal. The controller is tuned optimally by using a pattern search optimization method, and the gains are found to be $K_P = 0.15$, $K_I = 0.05$, and $K_D = 0.04$ [50], [51].

B. PI$^\lambda$D$^\mu$ Controller Design

The fractional-order PI$^\lambda$D$^\mu$ controller is a generalization of the integer-order PID controller exploiting the richness offered by the noninteger orders of the Laplace variable s. Denoting $C_C(s)$ as the transfer function associated to it, an analog PI$^\lambda$D$^\mu$ controller is described as given in the following [28]:

$$C_C(s) = \frac{U(s)}{E(s)} = K_p + K_i s^{-\lambda} + K_d s^{\mu}, (\lambda, \mu > 0) \quad (21)$$

where K_p is the proportional constant, K_i is the integration constant, and K_d is the differentiation constant. Clearly, for $\lambda = 1$ and $\mu = 1$, controller (21) takes the classical PID form. The performance of the PI$^\lambda$D$^\mu$ controller for the control of the considered manipulator is expected to be better than that of the classical PID controller due to its higher degrees of freedom for tuning.

According to their approximation methods, the dynamic behavior of fractional transfer functions can be classified into two subsections, either integer or digital transfer functions. The usefulness of such approximations may be summarized as follows.

1) While there are numerical methods to solve fractional differential equations, methods for integer differential equations are better known and are the ones widely available in commercial software.
2) While hardware implementations of fractional controllers are possible, it is often easier and cheaper to implement in hardware integer transfer functions only.

Additionally, frequency domain approaches and time domain approaches are other classification techniques for fractional-order PID controllers. It is possible to find seven main different design methodologies for the fractional-order PID controller in the literature.

These include the Crone approximation [32]–[34], Carlson approximation [52], Matsuda approximation [53], [54], Grünwald–Letnikoff approximation [41], truncated series approximations [41], [55]–[58], time response approximations [59], continuous approximations based on truncated continued fractions proposed by Vinagre [41], etc. [48], [60].

The fractional-order PID controller should ensure that the given gain crossover frequency and the phase margin are achieved and the phase derivative w.r.t. the frequency is zero, i.e., the phase Bode plot is flat, at the gain crossover frequency so that the closed-loop system is robust to gain variations and the step response exhibits an iso-damping property [61]. This expression is the summarization of the approach proposed by Bode and implemented by Manabe [48], [49]. Since most of the proposed methods for designing the fractional-order PID controller in the literature are based on this idea, in order to design the fractional-order PID controller for the considered system, the same idea and approach has been used in this study.

In order to determine the controller parameters K_p, K_i, K_d, λ, and μ, the transfer function of the system is required primarily.

As can be seen from (17)–(19), in order to make an effective control, the dc motor used to feed the Maryland manipulator mechanism should be controlled. As stated in (18) and (19), the torque value depends on both the armature current and angular velocity. Equation (17) determines the change of armature current in relation to angular velocity. According to (17), if the supply voltage is changed, then both the angular velocity and torque values are changed gradually. For this reason, the correct definition of the transfer function of the dc motor has very important effect on designating the fractional-order PI$^\lambda$D$^\mu$ controller. As defined in [48] and as can be seen from Fig. 5, the transfer function of the dc motor considered is in the form of the following expression:

$$G_{DC}(s) = \frac{\theta(s)}{V(s)} = \frac{K_t}{s\left[(Ls+R)(J_m s + B_m) + K_v K_t\right]}. \quad (22)$$

However, for many dc motors, the time constant of the armature is negligible [48], and therefore, we can simplify model (22). A simplified continuous mathematical model has the following form:

$$G_{DC}(s) = \frac{\theta(s)}{V(s)} = \frac{K_t}{s\left[R(J_m s + B_m) + K_v K_t\right]} = \frac{[K_t/(RB_m + K_v K_t)]}{s(\tau s + 1)} = \frac{K_M}{s(\tau s + 1)} \quad (23)$$

where the time constant $\tau = [RJ_m/(RB_m + K_v K_t)]$ and generalized motor time constant is $K_M = [K_t/(RB_m + K_v K_t)]$.

Using aforementioned constants for the selected motor, the transfer function (23) of the motor will be as the following

$$G_{DC}(s) = \frac{\theta(s)}{V(s)} = \frac{1.2325}{s(0.0407s + 1)}. \tag{24}$$

In order to design the fractional-order PI$^{\lambda}$D$^{\mu}$ controller (FOC) [48], an approach that has been proposed by Bode and described by Tustin [49] for the motion control will be used. This principle has also been used by Manabe in an induction motor speed control [49].

During the past ten years, in order to tune FOC parameters, several methods and tuning techniques based on various approaches were developed [26]–[44], [48].

We will design the controller which gives us a step response of the feedback control loop independent of payload changes (iso-damping). In the frequency domain point of view, it means the phase margin independent of the payload changes.

The phase margin of the controlled system is [48]

$$\Phi_m = \arg\left[C_C(\mathrm{j}\omega_{\mathrm{g}})G_{DC}(\mathrm{j}\omega_{\mathrm{g}})\right] + \pi \tag{25}$$

where $\mathrm{j}\omega_{\mathrm{g}}$ is the crossover frequency. In other words, independent phase margin means constant phase. This can be accomplished by the controller of the form

$$C_C(s) = k_1\frac{k_2 s + 1}{s^{\delta}} \quad k_1 = \frac{1}{K_M} \quad k_2 = \tau. \tag{26}$$

Such controller gives a constant phase margin, and the obtained phase margin is

$$\begin{aligned}\Phi_m &= \arg\left[C_C(\mathrm{j}\omega_{\mathrm{g}})G_{TMS}(\mathrm{j}\omega_{\mathrm{g}})\right] + \pi \\ &= \arg\left[(\mathrm{j}\omega_{\mathrm{g}})^{-(1+\delta)}\right] + \pi = \pi - (1+\delta)\frac{\pi}{2}.\end{aligned} \tag{27}$$

As given in [39] and [48], with regard to the general characteristics of Bode's ideal transfer function, the desired phase margin is $\Phi_m = 45^{\circ}$ for the considered mechanism. This is valid for only $\delta = 0.5$. With these constants, we obtain a fractional I$^{\lambda}$D$^{\mu}$ controller, which is a particular case of the PI$^{\lambda}$D$^{\mu}$ controller and has the form

$$C_C = 0.0502\sqrt{s} + \frac{0.8114}{\sqrt{s}}. \tag{28}$$

As well known, the behavior of the designed controller for the considered PMDC motor has to be ensured insensitive for changes in the load torque value. This property should also be provided for instantaneous changes for load torque. As can be seen from (14)–(16) and (18), the correct and effective control of the PMDC motor will also guarantee the exact and accurate control of the whole system.

In order to overcome the steady-state error, the integral component integrates the error over time. In addition, the derivative part of the PID algorithm anticipates the future behavior of the error because the response of the derivative component is proportional to the rate of change of the error. Therefore, in general, the derivative action prevents overshoot and eliminates oscillations. On the other hand, most practical control systems use very small derivative gain because the derivative response is highly sensitive to noise in the process variable signal.

Moreover, the proportional gain determines the ratio of output response to the error. In general, increasing the proportional gain will increase the speed of the control system response and also decrease the steady-state error which is the final difference between the process variable and set point.

As can be seen from (28), both integral and derivative terms are included in the controller transfer function. However, as mentioned earlier, in order to decrease the steady-state error value, a proportional gain has to be added. In order to determine this gain, a pattern search optimization method is also employed for the fractional-order PI$^{\lambda}$D$^{\mu}$ controller case. As can be seen from (28), the first term is a differentiator, and the second term of the equation is an integrator. K_I and K_D values are calculated from (28), and the K_P value is also considered as constant. According to (28), it is obvious that $K_D = 0.0502$ and $K_I = 0.8114$. After the pattern search optimization method, the proportional gain of the optimally tuned controller is found to be $K_P = 0.125$.

V. Results

As stated in (18) and (19), the produced magnetic torque using the PMDC motor provides the required torque values that are given in (14)–(16). The selected PMDC motor is a driver source for the manipulator load. In order to provide real system conditions, this type of connection has been considered and simulated. The input voltage of the PMDC motor has been controlled using the fractional-order PI$^{\lambda}$D$^{\mu}$ controller, and then, output torque has been applied to the manipulator.

According to this approach, a controller should be designed to regulate the position and angle fluctuations induced by the inertia effects and other disturbances that affect the system. In this paper, in the closed-loop fractional-order PI$^{\lambda}$D$^{\mu}$ control of the system, the inputs to the controller are the error, change of error, and integration of the error in the input link speed, and the output is the electromagnetic torque value determined with the aid of the supply voltage and armature current.

In order to examine the system, three different sequential trajectories have been considered as given in the following:

$$\left.\begin{aligned} p_x &= 0 \\ p_y &= 0 \\ p_z &= 0.35 + \tfrac{t^2}{1000} \end{aligned}\right\} \text{ if } t \le 5$$

$$\left.\begin{aligned} p_x &= 0.06\cos(t) \\ p_y &= 0.06\sin(t) \\ p_z &= 0.35 \end{aligned}\right\} \text{ if } 5 < t \le 10$$

$$\left.\begin{aligned} p_x &= 0 \\ p_y &= 0 \\ p_z &= 0.35 - \tfrac{t^2}{1000} \end{aligned}\right\} \text{ if } t > 10.$$

Using the previously defined trajectories, a dynamic analysis will be possible for the manipulator. The graphical representation of these trajectories for three axes is given in Fig. 6.

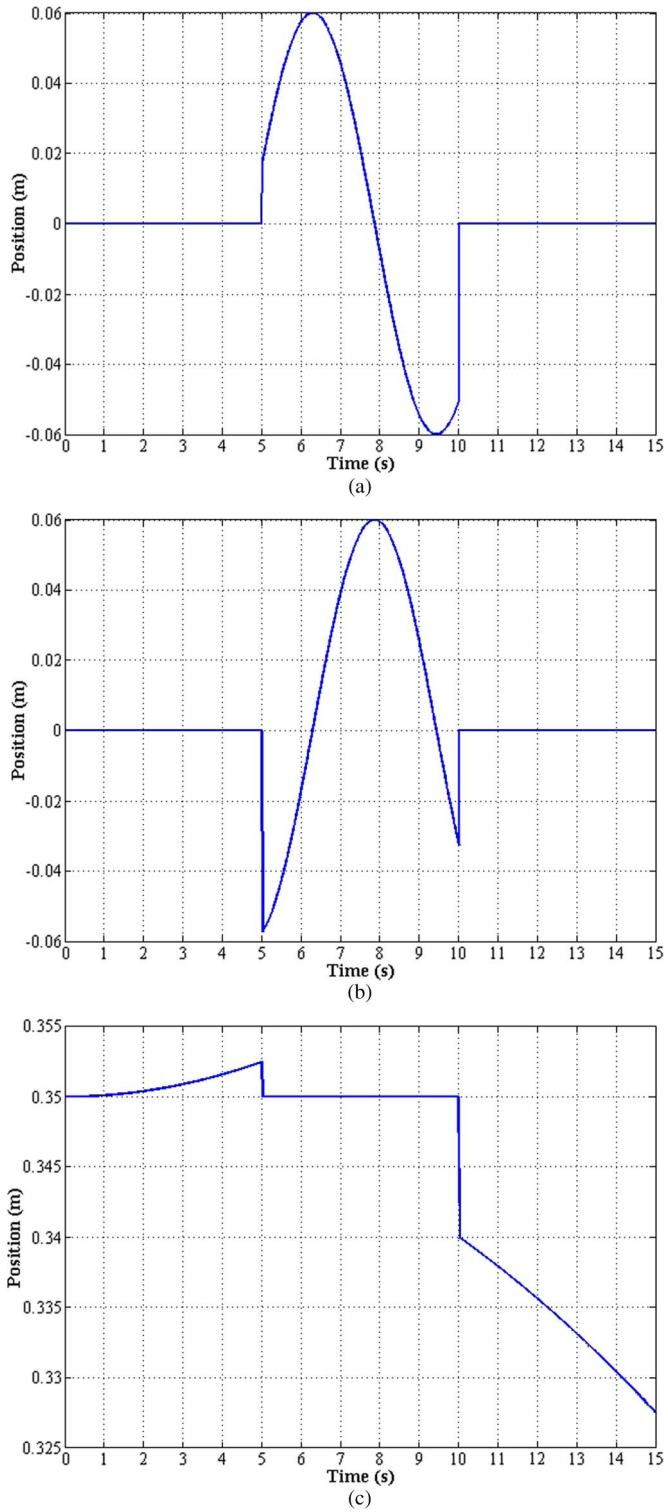

Fig. 6. Graphical representation of three trajectories for three axes. (a) x-axis. (b) y-axis. (c) z-axis.

The closed-loop step responses of the system for the given trajectories are given in Fig. 7 for an optimally tuned PID. Both the obtained torque value and desired torque value for the first motor are drawn in Fig. 7.

According to the desired and obtained torque values, the error graphic between these values is calculated and plotted in Fig. 8.

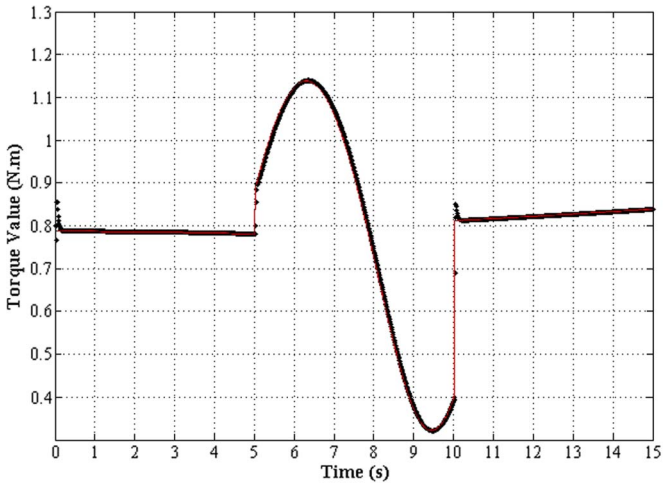

Fig. 7. Obtained and desired torque values for first motor for an optimally tuned PID. (-) Desired. (•) Obtained.

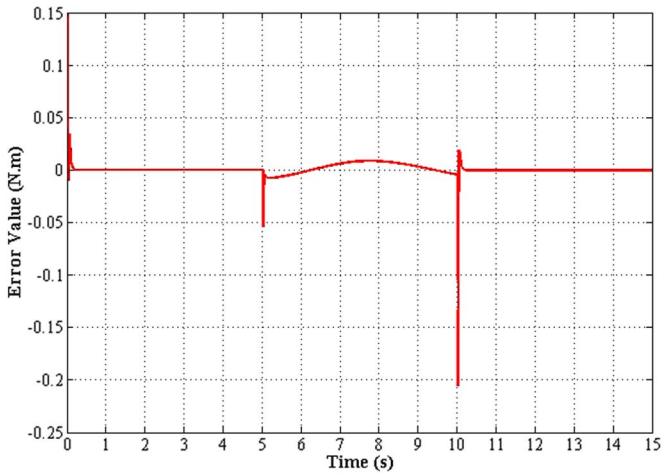

Fig. 8. Error graphic between obtained and desired torque values for optimally tuned PID.

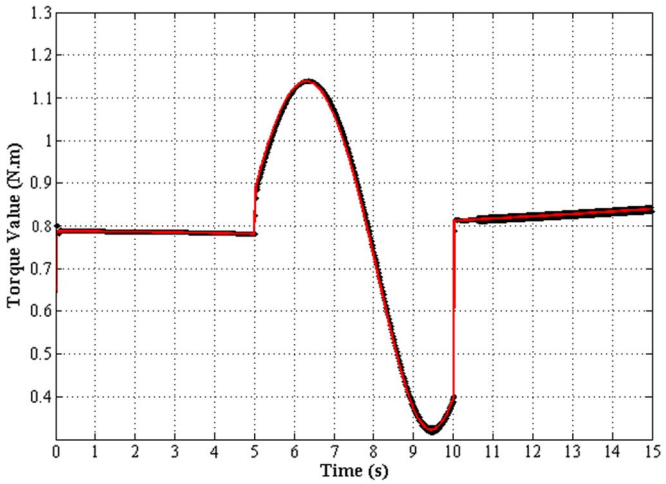

Fig. 9. Obtained and desired torque values for first motor for a fractional-order $PI^{\lambda}D^{\mu}$ controller. (-) Desired. (•) Obtained.

Using the fractional-order $PI^{\lambda}D^{\mu}$ controller, both obtained and desired torque values are also given in Fig. 9. The variation of the error graphic for the $PI^{\lambda}D^{\mu}$ controller case is illustrated in Fig. 10.

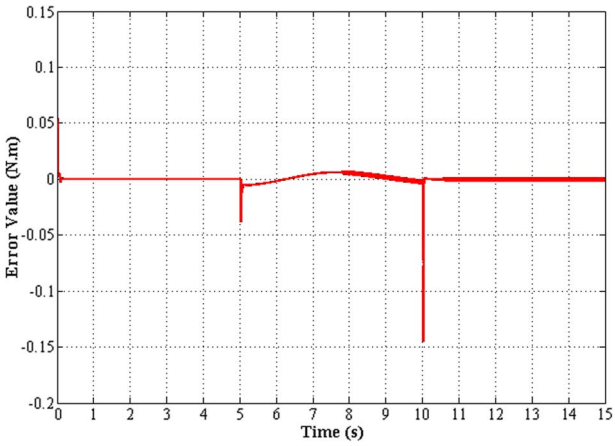

Fig. 10. Error graphic between obtained and desired torque values for fractional-order $PI^{\lambda}D^{\mu}$ controller case.

TABLE II
SSE AND MSE VALUES

Controller type	SSE value with respect to torque	SSE value with respect to angle	MSE value with respect to angle
Optimally tuned PID	20.63	5.6816	0.0038
Fractional order $PI^{\lambda}D^{\mu}$	7.96	0.8897	0.0006

As can be seen from Figs. 9 and 10, overshoot values are eliminated completely for the $PI^{\lambda}D^{\mu}$ controller case. In addition, both transient and steady-state error values are reduced by using the $PI^{\lambda}D^{\mu}$ controller.

In order to show the superiority of the $PI^{\lambda}D^{\mu}$ controller, SSE values with respect to both torque and angle values are tabulated in Table II for both cases.

As tabulated in Table II, the steady-state error value of the optimally tuned PID is greater than two times that of the fractional-order $PI^{\lambda}D^{\mu}$ controller. The mean squared error (MSE) value can also be used to illustrate the performance of the proposed controller. For this reason, MSE values are also tabulated in Table II as another performance criterion.

Additionally, in order to show the superiority of the $PI^{\lambda}D^{\mu}$ controller using another way, the error between the desired input link angle and obtained input link angle has been shown graphically and assessed in Figs. 11 and 12.

VI. CONCLUSION

The 3-DOF parallel manipulator known as the University of Maryland manipulator has been considered, and its tracking control for the given different trajectories has been studied. First, the dynamic model of the 3-DOF parallel manipulator has been introduced using the Tsai and Stamper method. Second, the mechanism and motor dynamic models are formulated. Then, in order to investigate the effect of different control approaches on the improvement of the tracking performance of the examined Maryland manipulator, two control approaches such as the classical PID and fractional-order PID control approaches have been considered. The classical PID controller

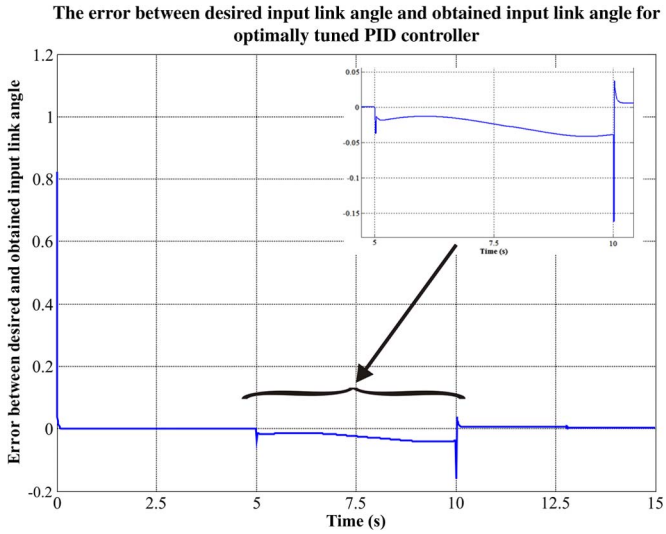

Fig. 11. Error graphic between desired input link angle and obtained input link angle for optimally tuned PID.

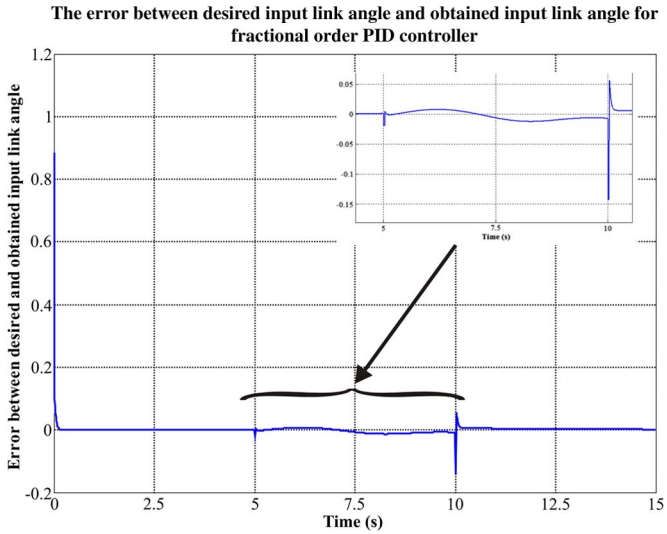

Fig. 12. Error graphic between desired input link angle and obtained input link angle for fractional-order $PI^{\lambda}D^{\mu}$ controller case.

has been tuned optimally by using a pattern search optimization method, and the gains have been found. Finally, design stages for the fractional-order $PI^{\lambda}D^{\mu}$ controller have been given in detail.

In order to examine the system, three different sequential trajectories have been considered, and results have been obtained for both cases. It is observed that overshoot values have been removed completely for the $PI^{\lambda}D^{\mu}$ controller case. Moreover, both transient and steady-state error values have been reduced by using the $PI^{\lambda}D^{\mu}$ controller. According to the SSE values between the desired and obtained torque values, obtained results for the fractional-order $PI^{\lambda}D^{\mu}$ controller are more superior than that of the optimally tuned PID.

In future, we would like to design an observer based on more complex controller structure for the considered manipulator. With the aid of the observer, it is expected that the error value for desired and obtained cases will be reduced.

REFERENCES

[1] D. Stewart, "A platform with six degrees of freedom," *Proc. Inst. Mech. Eng*, vol. 180, no. 1, pp. 371–386, Jun. 1965.

[2] Y. Li and Q. Xu, "Design and development of a medical parallel robot for cardiopulmonary resuscitation," *IEEE/ASME Trans. Mechatronics*, vol. 12, no. 3, pp. 265–273, Jun. 2007.

[3] M. Shoham, M. Burman, E. Zehavi, L. Joskowicz, E. Batkilin, and Y. Kunicher, "Bone-mounted miniature robot for surgical procedures: Concept and clinical applications," *IEEE Trans. Robot. Autom.*, vol. 19, no. 5, pp. 893–901, Oct. 2003.

[4] W. L. Xu, J. S. Pap, and J. Bronlund, "Design of a biologically inspired parallel robot for foods chewing," *IEEE Trans. Ind. Electron.*, vol. 55, no. 2, pp. 832–841, Feb. 2008.

[5] W. L. Xu, J. D. Torrance, B. Q. Chen, J. Potgieter, J. E. Bronlund, and J. S. Pap, "Kinematics and experiments of a life-sized masticatory robot for characterizing food texture," *IEEE Trans. Ind. Electron.*, vol. 55, no. 5, pp. 2121–2132, May 2008.

[6] E. Ottaviano and M. Ceccarelli, "Application of a 3-DOF parallel manipulator for earthquake simulations," *IEEE/ASME Trans. Mechatronics*, vol. 11, no. 2, pp. 241–246, Apr. 2006.

[7] K. M. Lee and S. Arjunan, "A three-degrees-of-freedom micromotion in parallel actuated manipulator," *IEEE Trans. Robot. Autom.*, vol. 7, no. 5, pp. 634–641, Oct. 1991.

[8] A. A. Ramadan, T. Takubo, Y. Mae, K. Oohara, and T. Arai, "Developmental process of a chopstick-like hybrid-structure two-fingered micromanipulator hand for 3-D manipulation of microscopic objects," *IEEE Trans. Ind. Electron.*, vol. 56, no. 4, pp. 1121–1135, Apr. 2009.

[9] F. J. Berenguer and F. M. M. Huelin, "Zappa, a quasi-passive biped walking robot with a tail: Modeling, behavior, and kinematic estimation using accelerometers," *IEEE Trans. Ind. Electron.*, vol. 55, no. 9, pp. 3281–3289, Sep. 2008.

[10] F. Pierrot, V. Nabat, O. Company, S. Krut, and P. Poignet, "Optimal design of a 4-DOF parallel manipulator: From academia to industry," *IEEE Trans. Robot.*, vol. 25, no. 2, pp. 213–224, Apr. 2009.

[11] T. Huang, D. G. Chetwynd, J. P. Mei, and X. M. Zhao, "Tolerance design of a 2-DOF overconstrained translational parallel robot," *IEEE Trans. Robot.*, vol. 22, no. 1, pp. 167–172, Feb. 2006.

[12] K. Liu, J. M. Fitzgerald, and F. L. Lewis, "Kinematics analysis of a Stewart platform manipulator," *IEEE Trans. Ind. Electron.*, vol. 40, no. 2, pp. 282–293, Apr. 1993.

[13] Z. M. Bi and Y. T. Lang, "Kinematic and dynamic models of a tripod system with a passive leg," *IEEE/ASME Trans. Mechatronics*, vol. 11, no. 1, pp. 108–111, Feb. 2006.

[14] D. Zhang and Z. Gao, "Optimal kinematic calibration of parallel manipulators with pseudoerror theory and cooperative coevolutionary network," *IEEE Trans. Ind. Electron.*, vol. 59, no. 8, pp. 3221–3231, Aug. 2012.

[15] L. C. T. Wang and M. J. Kuo, "Dynamic load-carrying capacity and inverse dynamics of multiple cooperating robotic manipulators," *IEEE Trans. Robot. Autom.*, vol. 10, no. 1, pp. 71–77, Feb. 1994.

[16] K. M. Lee and D. K. Shah, "Dynamic analysis of a three degrees of freedom in parallel actuated manipulator," *IEEE J. Robot. Autom.*, vol. 4, no. 3, pp. 570–578, Jun. 1988.

[17] P. Renaud, N. Andreff, J. M. Lavest, and M. Dhome, "Simplifying the kinematic calibration of parallel mechanisms using vision-based metrology," *IEEE Trans. Robot.*, vol. 22, no. 1, pp. 12–22, Feb. 2006.

[18] L. C. T. Wang and C. C. Chen, "On the numerical kinematic analysis of general parallel robotic manipulators," *IEEE Trans. Robot. Autom.*, vol. 9, no. 3, pp. 272–285, Jun. 1993.

[19] L. Ren, J. K. Mills, and D. Sun, "Trajectory tracking control for a 3-DOF planar parallel manipulator using the convex synchronized control method," *IEEE Trans. Control Syst. Technol.*, vol. 16, no. 4, pp. 613–623, Jul. 2008.

[20] Y. Su, D. Sun, L. Ren, and J. K. Mills, "Integration of saturated PI synchronous control and PD feedback for control of parallel manipulators," *IEEE Trans. Robot.*, vol. 22, no. 1, pp. 202–207, Feb. 2006.

[21] Y. X. Su, B. Y. Duan, and C. H. Zheng, "Nonlinear PID control of a six-DOF parallel manipulator," *Proc. Inst. Elect. Eng.—Control Theory Appl.*, vol. 151, no. 1, pp. 95–102, Jan. 2004.

[22] P. R. Ouyang, W. J. Zhang, and F. X. Wu, "Nonlinear PD control for trajectory tracking with consideration of the design for control methodology," in *Proc. IEEE Int. Conf. Robot. Autom.*, Washington, DC, USA, 2002, vol. 4, pp. 4126–4131.

[23] A. Müller and T. Hufnagel, "Model based control of redundantly actuated parallel manipulators in redundant coordinates," *Robot. Autom. Syst.*, vol. 60, pp. 563–571, Apr. 2011.

[24] F. H. Ghorbel, O. Chetelat, R. Gunawardana, and R. Longchamp, "Modeling and set point control of closed-chain mechanisms: Theory and experiment," *IEEE Trans. Control Syst. Technol.*, vol. 8, no. 5, pp. 801–815, Sep. 2000.

[25] Y. Li and Y. Wang, "Trajectory tracking control of a redundantly actuated parallel robot using diagonal recurrent neural network," in *Proc. Int. Conf. Natural Comput.*, 2009, pp. 292–296.

[26] S. E. Hamamci, "An algorithm for stabilization of fractional-order time delay systems using fractional-order PID controllers," *IEEE Trans. Autom. Control*, vol. 52, no. 10, pp. 1964–1969, Oct. 2007.

[27] F. M. Bayat and M. K. Ghartemi, "Method for designing $PI^{\lambda}D^{\mu}$ stabilisers for minimum-phase fractional-order systems," *IET Control Theory Appl.*, vol. 4, no. 1, pp. 61–70, Jan. 2010.

[28] M. Ö. Efe, "Neural network assisted computationally simple $PI^{\lambda}D^{\mu}$ control of a quadrotor UAV," *IEEE Trans. Ind. Informat.*, vol. 7, no. 2, pp. 354–361, May 2011.

[29] J. Han, "From PID to active disturbance rejection control," *IEEE Trans. Ind. Electron.*, vol. 56, no. 3, pp. 900–906, Mar. 2009.

[30] I. Podlubny, "Fractional-order systems and $PI^{\lambda}D^{\mu}$-controllers," *IEEE Trans. Autom. Control*, vol. 44, no. 1, pp. 208–214, Jan. 1999.

[31] Y. Luo, H. Chao, L. Di, and Y. Q. Chen, "Lateral directional fractional order $(PI)^{\alpha}$ control of a small fixed-wing unmanned aerial vehicles: Controller designs and flight tests," *IET Control Theory Appl.*, vol. 5, no. 18, pp. 2156–2167, Dec. 2011.

[32] A. Oustaloup, B. Mathieu, and P. Lanusse, "The CRONE control of resonant plants: Application to a flexible transmission," *Eur. J. Control*, vol. 1, no. 2, pp. 113–121, 1995.

[33] O. Altet, X. Moreau, M. Moze, P. Lanusse, and A. Oustaloup, "Principles and synthesis of hydractive CRONE suspension," *Nonlin. Dyn.*, vol. 38, no. 1/2, pp. 435–459, Dec. 2004.

[34] X. Moreau, O. Altet, and A. Oustaloup, "The CRONE suspension: Management of the dilemma comfort-road holding," *Nonlin. Dyn.*, vol. 38, no. 1/2, pp. 461–484, Dec. 2004.

[35] V. Feliu-Batlle, R. Perez, and L. Rodriguez, "Fractional robust control of main irrigation canals with variable dynamic parameters," *Control Eng. Pract.*, vol. 15, no. 6, pp. 673–686, Jun. 2007.

[36] J. Domingues, D. Valerio, and J. S. da Costa, "Rule-based fractional control of an irrigation canal," *ASME J. Comput. Nonlin. Dyn.*, vol. 6, no. 2, pp. 024503-1–024503-5, Oct. 2010.

[37] K. B. Oldham and J. Spanier, *The Fractional Calculus*. New York, NY, USA: Academic, 1974.

[38] K. S. Miller and B. Ross, *An Introduction to the Fractional Calculus and Fractional Differential Equations*. Hoboken, NJ, USA: Wiley, 1993.

[39] I. Podlubny, *Fractional Differential Equations: An Introduction to Fractional Derivatives, Fractional Differential Equations, to Methods of Their Solution and Some of Their Applications*. San Diego, CA, USA: Academic, 1999.

[40] A. A. Kilbas, H. M. Srivastava, and J. J. Trujillo, *Theory and Applications of Fractional Differential Equations*. Amsterdam, The Netherlands: Elsevier, 2006.

[41] D. Valerio and J. Sa da Costa, "Introduction to single-input, single-output fractional control," *IET Control Theory Appl.*, vol. 5, no. 8, pp. 1033–1057, May 2011.

[42] C. Yeroglu and N. Tan, "Note on fractional-order proportional–integral–differential controller design," *IET Control Theory Appl.*, vol. 5, no. 17, pp. 1978–1989, Nov. 2011.

[43] S. Saha, S. Das, R. Ghosh, B. Goswami, R. Balasubramanian, A. K. Chandra, S. Das, and A. Gupta, "Design of a fractional order phase shaper for iso-damped control of a PHWR under step-back condition," *IEEE Trans. Nucl. Sci.*, vol. 57, no. 3, pp. 1602–1612, Jun. 2010.

[44] S. Das, S. Das, and A. Gupta, "Fractional order modeling of a PHWR under step-back condition and control of its global power with a robust $PI^{\lambda}D^{\mu}$ controller," *IEEE Trans. Nucl. Sci.*, vol. 58, no. 5, pp. 2431–2441, Oct. 2011.

[45] L. W. Tsai and R. Stamper, "A parallel manipulator with only translational degrees of freedom," presented at the Proc. ASME, Design Engineering Tech. Conf., Irvine, CA, USA, 1996, 96-DETCMECH-1152.

[46] L.-W. Tsai, *Robot Analysis: The Mechanics of Serial and Parallel Manipulators*. Hoboken, NJ, USA: Wiley, 1999, pp. 134–142.

[47] R. Clavel, "Delta, A fast robot with parallel geometry," in *Proc. 18th ISIR*, Sydney, Australia, 1988, pp. 91–100.

[48] I. Petras, "Fractional-order feedback control of a dc motor," *J. Elect. Eng.*, vol. 60, no. 3, pp. 117–128, 2009.

[49] S. Manabe, "A suggestion of fractional-order controller for flexible spacecraft attitude control," *Nonlin. Dyn.*, vol. 29, no. 1–4, pp. 251–268, Jul. 2002.

[50] J. Tao and JP. Sadler, "Constant speed control of a motor driven mechanism system," *Mech. Mach. Theory*, vol. 30, no. 5, pp. 737–748, Jul. 1995.
[51] O. Gundogdu and K. Erenturk, "Fuzzy control of a dc motor driven four-bar mechanism," *Mechatronics*, vol. 15, no. 4, pp. 423–438, May 2005.
[52] G. E. Carlson and C. A. Hajlijak, "Approximation of fractional capacitors $(1/s)^{1/n}$ by a regular Newton process," *IEEE Trans. Circuit Theory*, vol. CT-7, no. 2, pp. 210–213, Jun. 1964.
[53] H. S. Wall, *Analytic Theory of Continued Fractions*. New York, NY, USA: Van Nostrand, 1948.
[54] W. H. Press, S. A. Teukolsky, and W. T. Vetterling, *Numerical Recipes in C: The Art of Scientific Computing*. Cambridge, U.K.: Cambridge Univ. Press, 1992.
[55] C. H. Lubich, "Discretized fractional calculus," *SIAM J. Math. Anal.*, vol. 17, no. 3, pp. 704–719, May 1986.
[56] J. A. T. Machado, "Analysis and design of fractional-order digital control systems," *J. Syst. Anal. Model. Simul.*, vol. 27, no. 2/3, pp. 107–122, 1997.
[57] J. A. T. Machado, "Discrete-time fractional-order controllers," *Fract. Calc. Appl. Anal.*, vol. 4, no. 1, pp. 47–66, 2001.
[58] Y. Q. Chen and B. Vinagre, "A new IIR-type digital fractional order differentiator," *Signal Process.*, vol. 83, no. 11, pp. 2359–2365, Nov. 2003.
[59] C. C. Tseng, "Design of fractional order digital FIR differentiators," *IEEE Signal Process. Lett.*, vol. 8, no. 3, pp. 77–79, Mar. 2001.
[60] G. Maione and P. Lino, "New tuning rules for fractional PIa controllers," *Nonlin. Dyn.*, vol. 49, no. 1/2, pp. 251–257, Jul. 2007.
[61] L. Hongsheng and C. Q. Yang, "A fractional order proportional and derivative (FOPD) controller tuning algorithm," in *Proc. Chin. Control Decis. Conf.*, 2008, pp. 4059–4063.

Ahmet Dumlu (M'12) was born in Erzurum, Turkey, in 1980. He received the B.S. degree from Erciyes University, Kayseri, Turkey, in 2004 and the M.S. degree from Ataturk University, Erzurum, in 2009, where he is currently working toward the Ph.D. degree.

His research interests include the theory of mechatronic and robotic systems, with a focus on observation and estimation-based control.

Koksal Erenturk (M'08) was born in Erzurum, Turkey, in 1973. He received the B.S. degree (with honors) in electrical engineering from Yildiz Technical University, Istanbul, Turkey, in 1994, the M.S. degree in electrical engineering from Istanbul University, Istanbul, in 1997, and the Ph.D. degree in electrical engineering from Karadeniz Technical University, Trabzon, Turkey, in 2002.

He is currently an Associate Professor with the Department of Electrical and Electronics Engineering, College of Engineering, Ataturk University, Erzurum. His work has focused on the development and application of control theory to a variety of mechatronic systems, with a focus on observation and estimation-based control. Much of his recent work has focused on the analysis and control of dynamical systems that arise in engineering applications. His areas of interest also include fuzzy logic and fuzzy control, neural networks, genetic algorithms, and their applications to dynamic systems and electrical engineering.